arXiv:hep-ph/9408240v3 5 Oct 1994

# Production of heavy bound states at LEP and beyond[1,2]

Arnd Leike[a] and Reinhold Rückl[a,b]

[a]*Sektion Physik der Universität München,*
*Theresienstr. 37, D–80333 München, FRG*
[b]*Max-Planck-Institut für Physik, Werner-Heisenberg-Institut,*
*Föhringer Ring 6, D–80805 München, FRG*

## Abstract

We describe some characteristic properties of $B_c$ mesons and discuss the production and the prospects of detection in $e^+e^-$, $\gamma\gamma$, and $\bar{p}p/pp$ collisions. The production mechanisms considered here also play an important role in charmonium and bottomonium production.

# 1 INTRODUCTION

With the production of $10^7$ $Z$ bosons at LEP rare Z decays with branching ratios as low as $10^{-6}$ come into experimental reach. Among these are decays into heavy quark bound states,

$$Z \to n^{2S+1}L_J + \text{ anything,} \tag{1}$$

where the usual spectroscopic notation is used. Particularly interesting is the possibility to produce bottom–charm bound states, so–called $B_c$ mesons. These states have not yet been discovered. They are the only quarkonium states with open heavy flavour quantum numbers, since the top quark is expected to be too heavy to form $T_c$ and $T_b$ resonances before it decays via $t \to bW^+$. Moreover, $B_c$ mesons constitute an excellent laboratory for studying QCD bound state dynamics, weak decay mechanisms, quark and gluon fragmentation, and hadronic matrix elements. All this provides strong motivation to investigate the prospects for observing $B_c$ mesons in present and future experiments.

In the following we briefly describe some characteristic properties of $B_c$ mesons, discuss the dominant production mechanisms in $e^+e^-$, $\gamma\gamma$, and $\bar{p}p/pp$ collisions, and indicate the prospects for detection of these new bound states.

# 2 SPECTROSCOPY

The energy levels and other spectroscopic properties of the $[\bar{b}c]$ system can be calculated in nonrelativistic potential models or with the help of QCD sum rules. Since the $B_c$ resonances lie in the mass range between charmonium and bottomonium, the predictions in a given approach are constrained by the latter systems. Thus, measurements of $B_c$ properties provide interesting tests of potential models and sum rule methods.

| MeV | Martin | BT | moment SR |
|---|---|---|---|
| $m_{B_c}$ | 6247 | 6272 | 6240-6320 |
| $m_{B_c^*} - m_{B_c}$ | 72 | 70 | 20-80 |
| $f_{B_c}$ | 511 | 442 | 410-440 |
| $f_{B_c^*} - f_{B_c}$ | 0 | 0 | 20-40 |

Table 1. Masses and decay constants [1] of the $^1S_0$ and $^3S_1$ ground states from potential models (Martin [2], BT [3]) and moment sum rules [4]. The normalization is such that $f_\pi = 132\,MeV$ and $f_{B_c^*} = f_{B_c}$ for nonrelativistic $S-$waves.

In table 1 we exemplify typical predictions for the pseudoscalar ($1^1S_0$) and vector ($1^3S_1$) ground states. While the mass predictions are very similar in different models and approaches, the decay constants are more distinctive (for reviews see e.g. [5]). Since the bound state wave functions are known in nonrelativistic approximation, one can also calculate more complicated quantities such as transition form factors and fragmentation functions, for example, for $B_c \to J/\psi$ and $\bar{b} \to B_c\bar{c}$. We will return to this possibility in section 4.

# 3 WEAK DECAYS

The weak decays of the lightest $B_c$ meson proceed via three distinct mechanisms: decay of the bottom constituent, decay of the charm constituent, and $\bar{b}c$ annihilation. In fact, the

free quark lifetimes, $\tau_b \simeq 1.5\,ps$ and $\tau_c \simeq 0.7\,ps$, are quite comparable, and also the lifetime $\tau_{\bar{b}c} \simeq 5.2\,ps$ due to the annihilation process is not very much longer. The interplay of these mechanisms should make $B_c$ decays rather unique and give rise to a rich and interesting decay pattern.

The decay widths corresponding to the above mechanisms have been estimated in quark models [6, 7] and using QCD sum rules [7, 8]. For the relative rates one finds

$$\Gamma_b : \Gamma_c : \Gamma_{\bar{b}c} \simeq \left\{ \begin{array}{ll} 37 : 45 : 18 & \text{potentials} \\ 48 : 39 : 13 & \text{sum rules.} \end{array} \right. \tag{2}$$

Deviations from the ratios $29 : 62 : 8$ of the above inverse lifetimes $\tau_b^{-1} : \tau_c^{-1} : \tau_{\bar{b}c}^{-1}$ are expected due to differences in the phase space available for the three decay channels. The total $B_c$ lifetime is estimated to lie in the range

$$\tau_{B_c} = 0.4 \div 0.9\,ps. \tag{3}$$

Decay modes with a $J/\psi$ resonance in the final state provide a particularly favourable signature for detection. Unfortunately, the branching ratios are only known with considerable uncertainties. For the most important channels one expects

$$Br(B_c \rightarrow J/\psi X) = \left\{ \begin{array}{ll} 2 \div 5\% & X = \bar{l}\nu_l \\ 0.2 \div 0.4\% & X = \pi \\ 0.6 \div 1.1\% & X = \rho. \end{array} \right. \tag{4}$$

The inclusive branching ratio for $B_c \rightarrow J/\psi X$ is about 20%. It should also be noted that the excited states below the open flavour threshold, $m_B + m_D \simeq 7.142\,GeV$, will all decay into the $B_c$ ground state via emission of photons, pions, etc., and hence contribute to the inclusive $B_c$ rate.

# 4  PRODUCTION IN $e^+e^-$ ANNIHILATION AND HEAVY QUARK FRAGMENTATION

In $e^+e^-$ annihilation $B_c$ mesons emerge from the simultaneous production of a $b\bar{b}$ and $c\bar{c}$ pair of quarks by strong binding of the $\bar{b}c$ pair in a colour–singlet state. (If no confusion can arise, both $B_c$ and $B_c^*$ are simply denoted by $B_c$.) The lowest–order Feynman diagrams of this process are shown in Fig. 1. Because of the nonrelativistic nature of $[\bar{b}c]$ bound states, the relative momentum $p$ of the $\bar{b}$ and $c$ quarks is expected to be small in comparison to the quark masses. It is then reasonable to expand the amplitudes in $p$, and to keep only the lowest nonvanishing term [9]. In this approximation, the amplitudes for the production of $S$–waves reduce to hard scattering amplitudes multiplied by the $S$–wave function $\Psi(0)$ at the origin. Similarly, for $P$–waves one obtains a product involving the derivative of the $P$–wave function. These wave functions can be estimated from potential models. For $S$–waves one can also substitute $\Psi(0)$ by the corresponding decay constants, $|\Psi(0)| = \sqrt{m_{B_c}/12}f_{B_c}$, and use for the latter the QCD sum rules estimates indicated in Table 1.

Straightforward calculation of the Feynman diagrams of Fig. 1 [10] then yields the total $B_c$ and $B_c^*$ cross sections exhibited in Fig. 2. As can be seen, below the $Z$ peak the cross sections amount to a few femtobarns only. At the resonance they reach about $1 \div 2\,pb$ corresponding

to $300 \div 500$ events for $10^7$ $Z$ bosons produced. Above the resonance the cross sections again drop rapidly below the level of 1 fb at LEP200. The production process considered here dominates other possible mechanisms such as soft fragmentation, that is nonperturbative creation of a heavy quark pair from the vacuum, and $W$–radiation from light fermions followed by $W^* \to \bar{b}c \to B_c$. The calculation can be drastically simplified for the following two reasons: Firstly, the minimum virtuality $k^2$ of the gluons in Fig. 1 is determined by the mass of the secondary quark pair, i.e. $k^2 \geq 4m_c^2$ in 1a and b, and $k^2 \geq 4m_b^2$ in 1c and d. Therefore, the gauge invariant subset of diagrams, 1a and b, is expected to yield the dominant contribution. Indeed, at $\sqrt{s} \geq 80 GeV$ the diagrams 1c and d contribute less than 5% as can be seen from Fig. 3. Secondly, in a planar gauge such as $Q^\mu G_\mu = 0$, where $Q^\mu = (p_{e^+} + p_{e^-})^\mu$ and $G^\mu$ denotes the gluon field, the contribution from diagram 1b is suppressed relative to that from diagram 1a. Again, this is demonstrated in Fig. 3. Consequently, for $s \gg m_{B_c}^2$ the complete process can be described to a very good approximation as production and fragmentation of $b$ quarks, $e^+e^- \to b\bar{b}$, $\bar{b} \to B_c\bar{c}$. This feature has been exploited in [11, 12, 13].



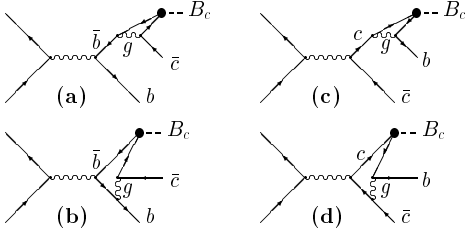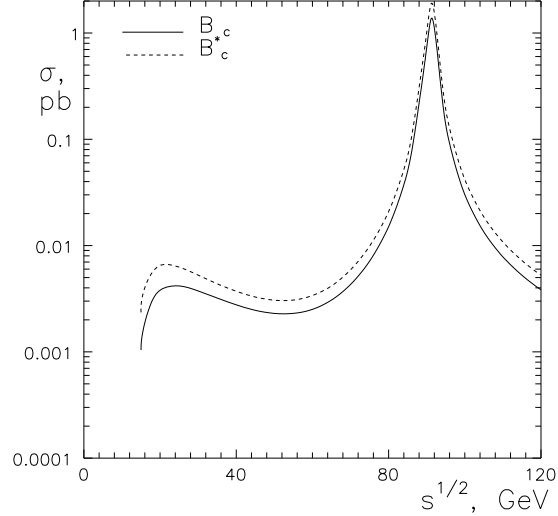**Fig. 1.** *The lowest–order Feynman diagrams contributing to $e^+e^- \to B_c b\bar{c}$.*

**Fig. 2.** *The total cross sections for $e^+e^- \to B_c^{(*)} b\bar{c}$ versus the c.m. energy.*

Following [12], we write the differential $B_c$ cross section as a convolution of the corresponding $b\bar{b}$ cross section and a fragmentation function:

$$d\sigma_{B_c}(E) = \int_0^1 dz d\sigma_{b\bar{b}}\left(\frac{E}{z}, \mu\right) D_{b \to B_c}(z, \mu), \tag{5}$$

where $\mu$ is the factorization scale and $z = 2E_{B_c}/\sqrt{s}$. For $\mu = O(m_{B_c})$ the fragmentation function can be calculated directly in QCD perturbation theory employing the nonrelativistic approximation sketched earlier. However, in order to avoid large corrections proportional to $ln\frac{E}{\mu}$ in $d\sigma_{b\bar{b}}$, it is necessary to take $\mu = O(E)$ and to evolve the fragmentation function $D_{\bar{b} \to B_c}$ from $\mu \simeq m_{B_c}$ to $\mu \simeq E$ using Altarelli–Parisi equations. To leading order, one has

$$\frac{\partial D_{\bar{b} \to B_c}(z, \mu)}{\partial ln \mu^2} = \frac{\alpha_s(\mu)}{2\pi} \int_z^1 \frac{dy}{y} P_{\bar{b}\bar{b}}\left(\frac{z}{y}\right) D_{\bar{b} \to B_c}(y, \mu)$$

4

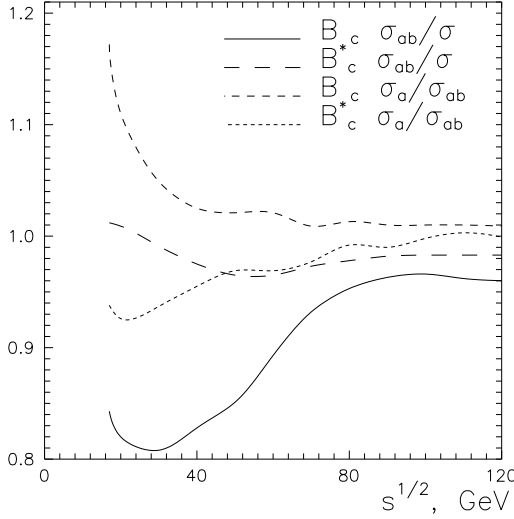$$\text{with } P_{\bar{b}b}(x) = \frac{4}{3}\left[\frac{1+x^2}{(1-x)_+} + \frac{3}{2}\delta(1-x)\right]. \tag{6}$$

**Fig. 3.** *Cross section ratios calculated from Figs. 1a–d ($\sigma$), 1a and b ($\sigma_{ab}$), and 1a alone in planar gauge ($\sigma_a$).*
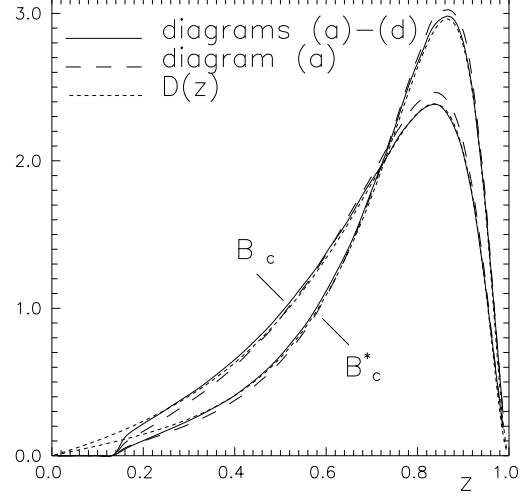
**Fig. 4.** *Energy distributions $\frac{d\sigma}{\sigma dz}$ calculated from diagrams 1a–d (solid line), and from diagram 1a alone in planar gauge (dashed line) in comparison to the fragmentation functions $D(z)$ given in (8), normalized to unity.*

Fig. 4 shows the fragmentation functions at $\mu = m_{B_c}$ for $\bar{b} \to B_c$ and $\bar{b} \to B_c^*$ normalized to unity in comparison to the distributions $\frac{1}{\sigma}\frac{d\sigma}{dz}$ as calculated from the complete set of diagrams in Fig. 1, and from Fig. 1a only. With the exception of the threshold behaviour at $z \to 0$, the direct calculation of $D_{\bar{b} \to B_c^{(*)}}$ provides an excellent approximation. Evolution to higher scales softens these distributions. This is exemplified in [12] for $\mu = 10 m_{B_c}$. However, since $\int_0^1 dz\, P_{\bar{b}b}(z) = 0$, the integrated fragmentation functions are not affected by evolution. Consequently, the branching fractions for $\bar{b} \to B_c^{(*)}\bar{c}$ are universal and scale independent numbers [12]:

$$BR\left(\bar{b} \to B_c^{(*)}\bar{c}\right) = \begin{cases} 2.2 \cdot 10^{-4} & (B_c) \\ 3.1 \cdot 10^{-4} & (B_c^*), \end{cases} \tag{7}$$

where $\alpha_s(m_{B_c}^2) = 0.2$ has been used. The fragmentation functions for $P$–waves have been worked out in [14].

It is instructive to compare the perturbative result:

$$D_{\bar{b} \to B_c^{(*)}}(z, \mu) = N_{B_c^{(*)}}(\mu, m_c)\frac{z(1-z)^2}{(1-r_b z)^6}F_{B_c^{(*)}}(z, d),$$

$$F_{B_c}(z, d) = \frac{z^4}{16}(1 + 2d + 2d^2 + 2d^3 + d^4) - \frac{z^3}{12}(2 + 3d + 10d^2 + 9d^3)$$

$$+ \frac{z^2}{6}(1 + 3d + 17d^2) - 3zd + 1,$$

5

$$F_{B_c^*}(z, d) = \frac{z^4}{16}(5 + 10d + 6d^2 + 2d^3 + d^4) - \frac{z^3}{4}(8 + 7d + d^3)$$

$$+\frac{z^2}{2}(9 - 3d + 3d^2) - z(2 + d) + 1, \tag{8}$$

where $d = (m_b - m_c)/(m_b + m_c)$, and $r_b = m_b/(m_b + m_c)$, with the phenomenological parametrization introduced in [15] for $D$ and $B$ meson fragmentation functions:

$$D(z) = N\frac{z(1 - z)^2}{[(1 - z)^2 + \epsilon z]^2}. \tag{9}$$

Here, the shape parameter $\epsilon$ is considered to be of order $m_q^2/m_Q^2$, $q$ and $Q$ denoting the light and heavy constituent quarks, respectively. Interestingly, for $\epsilon \simeq m_c^2/4m_b^2$ the parametrization (9) also provides a quite reasonable description of the distributions (8). In addition to the effective shape parameter $\epsilon$, perturbation theory predicts the absolute normalization,

$$N_{B_c^{(*)}}(\mu, m_c) = \frac{4\alpha_s^2(\mu^2)f_{B_c^{(*)}}^2}{81m_c^2}, \tag{10}$$

and the dependence on spin and orbital angular momentum [11, 12, 13, 14].

# 5 EVENT RATES AT THE Z POLE

In the fragmentation picture it is easy to estimate the total number of $B_c$ mesons produced at the $Z$ pole. One simply has to multiply the branching fraction $BR(Z \to b\bar{b}) = 0.152$ with the fragmentation probability of $b$ quarks into $B_c$ mesons. Since the excited states below the BD-threshold eventually decay into $B_c$ mesons, they have also to be counted. Adding up the $S$–waves, one obtains [12]

$$BR(\bar{b} \to B_c\bar{c}X) \approx 9 \cdot 10^{-4}. \tag{11}$$

One should, however, bear in mind the considerable uncertainties in this number. These are mainly due to the parameters appearing in the normalization factor (10), i. e. the scale $\mu$ in $\alpha_s$, the quark masses and the bound state wave functions or, equivalently, the decay constants. Combined, there is certainly a factor two uncertainty in (11) as can be seen from the varying predictions in the literature [11, 12, 13]. From the branching fractions given above one expects about

$$2700 \ B_c/\bar{B}_c \ \text{ per } \ 10^7 \ Z. \tag{12}$$

About 20% of these decay into final states containing a $J/\psi$. In turn, 12% of the $J/\psi$ resonances decay leptonically into $e^+e^-$ or $\mu^+\mu^-$. Hence, inclusively, one can expect roughly 60 events per $10^7$ $Z$ in the channel $B_c \to J/\psi X$; $J/\psi \to l^+l^-$. It should not be too difficult to observe such final states. Unfortunately, the $B_c$ signature will be obscured by a large background of $J/\psi$ events from other sources. Most importantly, one expects more than 3000 events per $10^7$ $Z$ from $Z \to b\bar{b}$; $b/\bar{b} \to J/\psi X$; $J/\psi \to l^+l^-$, where we have assumed an inclusive branching ratio of 1% for $b \to J/\psi$ X and the same for $\bar{b}$. This clearly shows that in order to discriminate the $B_c$ events from the background one has to tag the charm quark jet accompanying the $[\bar{b}c]$ bound states in $Z \to b\bar{b}$; $\bar{b} \to {}^{2S+1}L_J\bar{c}$; ${}^{2S+1}L_J \to B_cX$; $B_c \to J/\psi X$.

Alternatively, one may search for the $B_c$ meson in the particularly clean detection channels $B_c \to J/\psi l^+\nu_l$ and $B_c \to J/\psi \pi^+$. Using the range of branching fractions given in (4), one can expect $6 \div 16$ events for $10^7$ $Z$ in the channel $l^+l^-l^+\nu_l$ and a few events in the channels $l^+l^-\pi^+$ and $l^+l^-\rho^+$. These rates are small, but maybe just sufficient for $B_c$ discovery.

# 6  $B_c$ AT HADRON COLLIDERS

Given the abundant production rates of $b$–quarks in hadronic collisions, the prospects for detecting the $B_c$ mesons at the TEVATRON or LHC should look much better. In addition to the small fragmentation probabilities for $\bar{b} \to B_c \bar{c}$, these rates also afford small $B_c$ branching ratios. The by far dominant subprocess is gluon–gluon fusion, $gg \to B_c \bar{c} b$, with a small contribution coming also from $q\bar{q}$ annihilation, $q\bar{q} \to B_c \bar{c} b$.

Unlike in the case of $e^+ e^-$ annihilation, only a minority of diagrams possesses the topology of fragmentation processes, e. g. $gg \to b\bar{b}$; $\bar{b} \to B_c \bar{c}$. Correspondingly, heavy quark fragmentation can only be expected to dominate $B_c$ production at large transverse momenta. At smaller $p_T$ and for total cross sections, recombination processes such as $gg \to b\bar{b}\, c\bar{c}$; $\bar{b}c \to B_c$ will play an important role. The onset of the asymptotic regime in $p_T$, where the fragmentation picture is valid, is a priori not clear. We will return to this point in the next section.

|  | $\sigma_{inc}$ | $\sigma_{dir}$(cuts) | $N_{inc}$(cuts) |
|---|---|---|---|
| TEVATRON | | $p_T > 10\,GeV,\ \|y\| < 1$ | |
| $(25\,pb^{-1})$ | $5.3\,\mathrm{nb}$ | $0.13\,\mathrm{nb}$ | $1.6 \cdot 10^4$ |
| LHC | | $p_T > 20\,GeV,\ \|y\| < 2.5$ | |
| $(100\,fb^{-1})$ | $60\,\mathrm{nb}$ | $0.5\,\mathrm{nb}$ | $2.1 \cdot 10^8$ |

Table 2. Cross sections and number of events at $\sqrt{s} = 1.8\,TeV$ (TEVATRON) and $14(16)\,TeV$ (LHC) for inclusive ($inc$) and direct ($dir$) $B_c$ production.

In Table 2 we quote estimates for cross sections and production rates which can be found in the literature. The total cross sections $\sigma_{inc}$ have been calculated in [16] taking into account the complete sets of $O(\alpha_s^4)$–Feynman diagrams for the $gg$ and $q\bar{q}$ subprocesses, and summing the individual cross sections for $1S$ and $2S$ waves. On the other hand, the high-$p_T$ cross sections $\sigma_{dir}(cuts)$ have been obtained in [17] using an approximation analogous to (5), and considering only direct fragmentation into the $B_c$ ground state described by (8). Also applied are usual rapidity cuts. We emphasize that the uncertainties in these predictions are even larger than in the case of $e^+ e^-$ annihilation. The main reason is the scale ambiguity in the QCD coupling constant which enters here in fourth power. This makes the evaluation of higher-order QCD corrections very desirable.

As anticipated, even at high $p_T$ the production rates are large enough to afford detection channels with branching ratios of order 1% and below. In fact, CDF has already recorded some candidate events [18]. A B-physics experiment at LHC should certainly be able to investigate the $B_c$ system in some detail.

# 7  PHOTON–PHOTON PRODUCTION – A THEORETICAL STUDY CASE

As pointed out, hadronic production of $B_c$ mesons involves fragmentation and recombination mechanisms and is thus more involved than $B_c$ production by $e^+ e^-$ annihilation. In order to learn about the relative importance of fragmentation and recombination and their distinctive features, we have investigated $B_c$ production in $\gamma\gamma \to B_c b\bar{c}$. This process is simpler than $gg$ fusion, but involves the same two mechanisms as can be seen from the Feynman diagrams in Fig. 5. Moreover, it is interesting to find out whether there is a chance to observe $B_c$ mesons in laser induced $\gamma\gamma$ collisions feasible at future linear collider facilities [19].

In Fig. 6 we compare the cross section derived from the complete set[3] of $O(\alpha^2\alpha_s^2)$ diagrams indicated in Fig. 5 with the result obtained from the gauge invariant subset (I), which includes the fragmentation diagrams. Also shown is the cross section resulting from a convolution of $\sigma(\gamma\gamma \to b\bar{b})$ with the fragmentation function $D_{\bar{b}\to B_c}$ in analogy to (5). We observe that the integrated cross section is dominated by the recombination mechanism. This is not unexpected. We also find agreement between the predictions of diagrams (I) and simple $b$−quark fragmentation. Apparently, there is a gauge in which the first diagram of set (I) dominates.
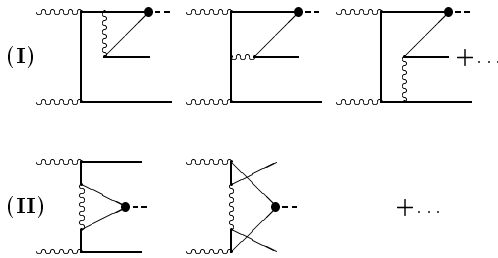


**Fig. 5.** *Different topologies of the lowest-order Feynman diagrams contributing to $\gamma\gamma \to B_c c\bar{b}$.*
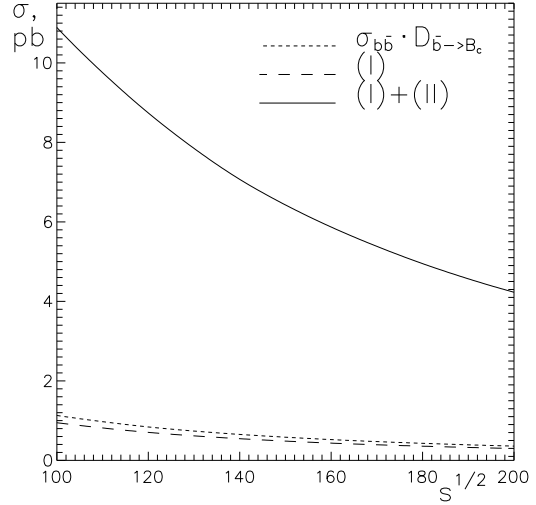
**Fig. 6.** *The total cross section for $\gamma\gamma \to B_c b\bar{c}$ as function of the c.m. energy.*

Furthermore, we have found that the energy distribution resulting from subset (I) is very similar to the distribution predicted by the pure fragmentation description. This is illustrated in Fig. 7 together with the complete energy distribution including also the recombination processes (II). The latter completely change the character of the energy spectrum giving rise to rather soft $B_c$ production.

We have also compared the corresponding $p_T$ distributions. As expected, the recombination processes mainly populate the low–$p_T$ region. Nevertheless, their $p_T$ spectrum has a long tail towards high $p_T$. For example, at $\sqrt{s} = 100\,GeV$ and $p_T = 20\,GeV$, the contribution from the diagrams (I) and (II) are still equally important. Recombination dies out completely only at $p_T \approx 40\,GeV$. These findings put some doubt on the estimates in [17] of $B_c$ production at high–$p_T$ in hadronic collisions, where the fragmentation approximation is used at $p_T \ll \sqrt{s}$.

In contrast to the energy and $p_T$ distributions, the angular distributions resulting from fragmentation and recombination processes are quite similar in shape. All distributions are sharply peaked for $|\cos\theta| \to 1$, with the distribution derived from the complete set of diagrams in Fig. 5 being somewhat flatter than the approximations from diagrams (I) and from $d\sigma_{b\bar{b}} \otimes D_{\bar{b}\to B_c}$.

As a final remark, for $\sqrt{s} \geq 100\,GeV$ we predict an integrated cross section below 12 fb.

---

[3]Diagrams of type (I) with the photons coupled to the $c$-quark line are not taken into account. They contribute an extra 15% to the total cross section [20]

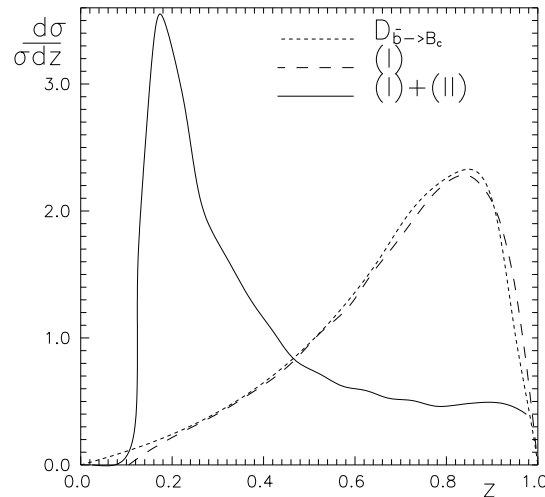This shows that $\gamma\gamma$ colliders cannot be expected to provide promising opportunities in $B_c$ physics.



**Fig. 7.** *Energy distributions calculated from the diagrams (I) and (II) of Fig. 5, and from the subset (I) alone in comparison to the fragmentation function $D_{\bar{b} \to B_c}(z, \mu)$ given in (8), normalized to unity.*

## 8 SUMMARY

The $B_c$ system provides plenty of possibilities to investigate interesting aspects of strong and weak interactions. Most importantly, the quarkonium nature of these bound states allows to calculate and study also genuinely nonperturbative quantities such as total cross sections, decay amplitudes, transition form factors and decay constants. Therefore, $B_c$ physics can serve as a testing ground for quantitative theoretical approaches to confinement problems. Practically, $B_c$ mesons are coming into experimental reach, may be at LEP, likely at the TEVATRON, but most certainly at LHC.

## References

[1] S. Reinshagen, diploma thesis, Univ. of Munich 1991; we are grateful to S. Reinshagen for providing the results of table 1.

[2] A. Martin, Phys. Lett. **B100** (1981) 511.

[3] W. Buchmüller, S.-H.H. Tye, Phys. Rev. **D24** (1981) 132.

[4] M.A. Shifman, A.I. Vainshtein, V.I. Zakharov, Nucl. Phys. **B147** (1979) 385; 448.

[5] W. Kwong, J.L. Rosner, Phys. Rev. **D44** (1991) 212; V.V. Kiselev, A.K. Likhoded, A.V. Tkabladze, IHEP 94-51; and references therein.

[6] Y.-Q. Chen, PhD thesis, Inst. of Theor. Phys., Academia Sinica, 1992; M. Lusignoli, M. Masetti, Z. Phys. **C51** (1991) 549.

[7] V.V. Kiselev, A.K. Likhoded, A.V. Tkabladze, Phys. At. Nucl. **56** (1993) 643; A.K. Likhoded et al., BARI-TH 93-137.

[8] P. Colangelo, G. Nardulli, N. Paver, Z. Phys. **C57** (1993) 43.

[9] B. Guberina, J.H. Kühn, R.D. Peccei, R. Rückl, Nucl. Phys. **B174** (1980) 317.

[10] L. Clavelli, Phys. Rev. **D26** (1982) 1610; C.-R. Ji, R. Amiri, Phys. Rev. **D35** (1987) 3318; V. Barger, K. Cheung, W.-Y. Keung, Phys. Rev. **D41** (1990) 1541; C.-H. Chang, Y.-Q. Chen, Phys. Lett. **B284** (1992) 127.

[11] F. Amiri, C.-R. Ji, Phys. Lett. **B195** (1987) 593; C.-H. Chang, Y.-Q. Chen, Phys. Rev. **D46** (1992) 3845.

[12] E. Braaten, K. Cheung, T.C. Yuan, Phys. Rev. **D48** (1993) 4230; R5049.

[13] A.F. Falk, et al. Phys. Lett. **B312** (1993) 486.

[14] Y.-Q. Chen, Phys. Rev. **D48** (1993) 5181.

[15] C. Peterson, D. Schlatter, I. Schmitt, P.M. Zerwas, Phys. Rev. **D27** (1983) 105.

[16] C.-H. Chang, Y.-Q. Chen, Phys. Rev. **D48** (1993) 4086.

[17] K. Cheung, Phys. Rev. Lett. **71** (1993) 3413.

[18] T. Müller (CDF Collaboration), Spring Meeting of the German Physical Society, Dortmund, Germany, March 1-4, 1994.

[19] V.I. Telnov, in Proc. of the IXth Int. Workshop on Photon-Photon Collisions, eds. D.O. Caldwell, H. P. Paar (World Scientific, Singapore, 1992) p. 369.

[20] K. Kołodziej, A. Leike, R. Rückl, in preparation.